Inorg. Chem. **2002**, *41*, 5693–5698

Ternary Nanoclusters of CuHgS, CuHgSe, and CuInS

Diem T. T. Tran,[†] Lianne M. C. Beltran,[†] Collin M. Kowalchuk,[†] Nicholas R. Trefiak,[†] Nicholas J. Taylor,[‡] and John F. Corrigan*[,†]

Departments of Chemistry, The University of Western Ontario, London, Ontario N6A 5B7, Canada, and University of Waterloo, Waterloo, Ontario N2L 3G1, Canada

Received October 12, 2001

Two copper–mercury–chalcogenide clusters $[Hg_{15}Cu_{20}E_{25}(PPr_3)_{18}]$ (**1**, E = S; **2**, E = Se) are synthesized in good yield from the reaction of $(Pr_3P)_3Cu–ESiMe_3$ and $(Pr_3P)_2{\cdot}Hg(OAc)_2$ at low temperatures. Single-crystal X-ray analyses illustrate that the two ternary clusters are isomorphous and consist of a phosphine-stabilized core of mixed Hg, Cu, and E centers. Thermolysis of **1** leads to the formation of mercury metal and various forms of copper–sulfide. The copper–indium–sulfide cluster $[Cu_6In_8S_{13}Cl_4(PEt_3)_{12}]$ (**3**) is similarly prepared in 50% yield from $(Et_3P)_3Cu–SSiMe_3$, $InCl_3$, and $S(SiMe_3)_2$.

Introduction

The continued interest in metal−chalcogenide (M−S, M−Se, M−Te) semiconductor colloidal and nanocluster materials and their possible uses in materials applications[1] have led to many efforts to access particles in a size-controlled manner, as exemplified with XII−XVI cluster/colloid synthesis.[2] Silyl chalcogen reagents offer excellent routes into XI−XVI nanoclusters with well-defined cores that are suitable for single-crystal X-ray analyses, and the development of this area of chemistry by Fenske and co-workers has led to the successful isolation of a large number of binary metal−chalcogenide nanoclusters, synthesized via the reaction of metal salts and $E(SiMe_3)_2$ (E = S, Se, Te), where the formed metal−chalcogenide cores are stabilized by phosphine ligands.[3] (Trimethylsilyl)seleno- and telluro-ethers (RE−$SiMe_3$, ArE−$SiMe_3$) can also be used for the generation of other series of novel high-nuclearity (metal−chalcogenide−chalcogenolate) clusters stabilized with selenolate[4] and tellurolate[5] surfaces.

To date the exploration of binary metal−sulfide and −selenide (ME) nanoclusters has been much more extensive in contrast to ternary (MM′E) nanoclusters,[6] and this may be attributed, in part, to a lack of suitable "binary" silyl

* To whom correspondence should be addressed. E-mail: corrigan@uwo.ca.

[†] The University of Western Ontario.

[‡] University of Waterloo.

(1) For selected recent reviews, see (a) Efros, Al. L.; Rosen, M. *Annu. Rev. Mater. Sci.* **2000**, *30*, 475−521. (b) Eychmüller A. *J. Phys. Chem. B* **2000**, *104*, 6514−6528 (c) Eychmüller A.; Rogach, A. l. *Pure Appl. Chem.* **2000**, *72*, 179−188. (d) Adair, J. H.; Li, T.; Kido, T.; Havey, K.; Moon. J.; Mecholsky, J.; Morrone, A.; Talham, D. R.; Ludwig, M. H.; Wang, L. *Mater. Sci. Eng.* **1998**, *R23*, 139−242. (e) Nirmal, M.; Brus, L. *Acc. Chem. Res.* **1999**, *32*, 407−414. (f) Herron, N.; Thorn, D. L. *Adv. Mater.* **1998**, *10*, 1173−1184. (g) Alivisatos, A. P. *J. Phys. Chem.* **1996**, *100*, 13226−13239. (h) Weller, H. *Angew. Chem., Int. Ed.* **1998**, *37*, 1658−1659. (i) Murphy, C. J. *J. Cluster Sci.* **1996**, *7*, 341−350.

(2) For examples of XII−XVI nanocluster and nanoparticle syntheses, see: (a) Green, M.; O'Brien, P. *Chem. Commun.* **1999**, 2235−2241. (b) Herron, N.; Wang, Y.; Eckert, H. *J. Am. Chem. Soc.* **1990**, *112*, 1322−1326. (c) Dance, I. G.; Choy, A.; Scudder, M. L. *J. Am. Chem. Soc.* **1984**, *106*, 6285−6295. (d) Herron, N.; Calabrese, J. C.; Farneth, W. E.; Wang, Y. *Science* **1993**, *259*, 1426−1428. (e) Steigerwald, M. L.; Alivisatos, A. P.; Gibson, J. M.; Harris, T. D.; Kortan, R.; Muller, A. J.; Thayer, A. M.; Duncan, T. M.; Douglass, D. C.; Brus, L. E. *J. Am. Chem. Soc.* **1988**, *110*, 3046−3050. (f) Murray, C. B.; Norris, D. J.; Bawendi, M. G. *J. Am. Chem. Soc.* **1993**, *115*, 8706−8715. (g) Vossmeyer, T.; Reck, G.; Katsikas, L.; Haupt, E. T. K.; Schulz, B.; Weller, H. *Science* **1993**, *267*, 1476−1479. (h) Adams, R. D.; Zhang, B.; Murphy, C. J.; Yeung, L. K. *Chem. Commun.* **1999**, 383−384. (i) Vossmeyer, T.; Reck, G.; Schulz, B.; Katsikas, L.; Weller, H. *J. Am. Chem. Soc.* **1995**, 117, 12881−12882. (j) Soloviev, V. N.; Eichhöfer, A.; Fenske, D.; Banin, U. *J. Am. Chem. Soc.* **2001**, *123*, 2354−2364. (k) Rogach, A. L.; Kornowski, A.; Gao, M. Y.; Eychmüller, A.; Weller, H. *J. Phys. Chem. B* **1999**, *103*, 3065−3069. (l) Talapin, D. V.; Haubold, S.; Rogach, A. L.; Kornowski, A.; Haase, M.; Weller, H. *J. Phys. Chem. B* **2001**, *105*, 2260−2263.

(3) (a) Eichhöfer, A.; Corrigan, J. F.; Fenske, D.; Tröster, E. *Z. Anorg. Allg. Chem.* **2000**, *626*, 338−348. (b) Dehnen, S.; Fenske, D. *Chem.−Eur. J.* **1996**, *2*, 1407−1416. (c) Eichhöfer, A.; Fenske, D. *J. Chem. Soc., Dalton Trans.* **1998**, 2969−2972. (d) Dehnen, S.; Schäfer, A.; Ahlrichs, R.; Fenske, D. *Chem.−Eur. J.* **1996**, *2*, 429−435. (e) Deveson, A.; Dehnen, S.; Fenske, D. *J. Chem. Soc., Dalton Trans.* **1997**, 4491−4497. (f) Fenske, D.; Krautscheid, H.; Balter, S. *Angew. Chem., Int. Ed. Engl.* **1990**, *29*, 796−799. (g) Fenske, D.; Steck, J.-C. *Angew. Chem., Int. Ed. Engl.* **1993**, *32*, 238−240. (h) Krautscheid, H.; Fenske, D.; Baum, G.; Semmelmann, M. *Angew. Chem., Int. Ed. Engl.* **1993**, *32*, 1303−1305.

(4) (a) Bettenhausen, M.; Eichhöfer, A.; Fenske, D.; Semmelmann, M. *Z. Anorg. Allg. Chem.* **1999**, *625*, 593−601. (b) Zhu, N.; Fenske, D. *J. Chem. Soc., Dalton Trans.* **1999**, 1067−1075. (c) Eichhöfer, A.; Fenske, D.; Pfistner, H.; Wunder, M. *Z. Anorg. Allg. Chem.* **1998**, *624*, 1909−1914. (d) Fenske, D.; Zhu, N.; Langetepe, T. *Angew. Chem., Int. Ed.* **1998**, *37*, 2639−2644.

10.1021/ic0110528 CCC: $22.00
Published on Web 10/02/2002

reagents that can be employed to yield ternary clusters. A general molecular synthetic route to access ternary nanoclusters is desirable since ternary materials find widespread applications in optical and electronic devices. For example $Hg_{1-x}Cd_xTe$ ($x = 0-1$) has been used in IR detection[7] and $CuInS_2$ ($E_g = 1.5$ eV) semiconducting thin films display desirable properties for use in solar cells applications.[8]

We communicated recently[9] that tris(tripropylphosphine)-copper (trimethylsilyl thiolate), $(Pr_3P)_3Cu-SSiMe_3$, may be used as a soluble source of "copper thiolate", "CuS^-", in the formation of a mercury−copper−sulfide cluster. Herein we describe the detailed synthesis and properties of the ternary clusters $[Hg_{15}Cu_{20}S_{25}(PPr_3)_{18}]$ (**1**), $[Hg_{15}Cu_{20}Se_{25}(PPr_3)_{18}]$ (**2**), and $[Cu_6In_8S_{13}Cl_4(PEt_3)_{12}]$ (**3**) using the complexes $(R_3P)_3Cu-ESiMe_3$ (R = Pr, Et; E = S, Se).[10]

Results and Discussion

Due to the labile nature of the phosphine ligands bonded to the copper center, in conjunction with the expected reactivity of the $E-SiMe_3$ moiety, we reasoned that the chalcogenolate reagents synthesized, $(R_3P)_3Cu-ESiMe_3$, would serve as a good source of "metallachalcogenolate" $Cu-E^-$, when reacted with a second metal salt. The complexes $(R_3P)_3Cu$-$ESiMe_3$ [**4a**, R = Pr, E = S; **4b**, R = Pr, E = Se; **5**, R = Et, E = S) are prepared in good yield from the 1:1 reaction of $(R_3P)_3Cu-OAc$ and $E(SiMe_3)_2$ at low temperatures.[10] Thus, when **4a** is treated with 0.5 equiv of $(Pr_3P)_2{\cdot}Hg(OAc)_2$ at −75 °C, orange crystals of $[Hg_{15}Cu_{20}S_{25}(PnPr_3)_{18}]$ (**1**) (60% yield) formed after a few hours at −30 °C (eq 1). These crystals seem to be photosensitive in that they darken to a black color upon exposure to direct light and are best stored under an inert atmosphere in the absence of visible light. Crystals of **1** are otherwise stable and dissolve in common polar organic solvents with the addition of excess tripropylphosphine. An X-ray analysis reveals that **1** is a "pinwheellike" ternary complex with Hg, Cu, and S centers interspersed in the structure of the $0.7 \times 1.2 \times 1.2$ nm^3 core. The structural details for **1** have been reported in some detail[9] and are not repeated here. The use of different phosphines ($PPhEt_2$ and PPh_2Et) to solubilize $Hg(OAc)_2$ before reaction with **4a** affords only **1**, thus illustrating that the phosphine ligands in the cluster originate from the chalcogenolate reagent. Although the ratio of Hg:Cu:S in **1** is 3:4:5, versus the 3:6:6 ratio of these elements in the reaction mixture, the preformed S−Cu bond in **4a** is required for the formation of **1**, as simple mixtures of 1:0.5:5 $CuOAc:Hg(OAc)_2:PPr_3$ and $S(SiMe_3)_2$ do not generate the ternary cluster. This contrasts with the synthetic route to the recently reported copper−indium−selenide clusters, such as $[Cu_6In_8Se_{13}Cl_4(P^nPr_2Ph)_{12}]$ (vide infra) which is prepared from mixing CuCl, $InCl_3$, and $Se(SiMe_3)_2$.[6a]

$$(Pr_3P)_3Cu-ESiMe_3 + 0.5Hg(OAc)_2{\cdot}2PPr_3 \xrightarrow[-75 \rightarrow -30\ ^\circ C]{THF} [Hg_{15}Cu_{20}E_{25}(PPr_3)_{18}]\ (E = S\ (\mathbf{1}),\ Se\ (\mathbf{2})) + OAcSiMe_3 + PPr_3 \quad (1)$$

Phosphine-stabilized mercury−chalcogenide (-olate) and related clusters, most of which are lower nuclearity complexes such as $[Hg_6(SePh)_{12}(PtBu_3)_2]$,[11a] display adamantoid frameworks.[11] The nanocluster $[Hg_{32}Se_{14}(SePh)_{36}]$, which has a metal core consisting of fused adamantane cages, has been reported and was shown to be a good example of a cluster displaying the size quantization effect.[12] The solid-phase diffuse reflectance UV−vis analysis of **1** displays a broad, featureless absorption profile starting at ∼750 nm with no distinct maximum. This type of absorption profile is characteristic of other copper(I)−chalcogenide nanocluster complexes.[3a]

When a solution of **1** is refluxed in toluene at 110 °C for 3 h, a clear, colorless solution results with the concomitant formation of a black powder and beads of mercury metal. GC-MS analysis of the volatiles from this treatment indicates the presence of only $S{=}PPr_3$. Components of the black powder consisted of HgS, Cu_2S, $Cu_{1.96}S$, $Cu_{2-x}S$, and $Cu_{7.2}S_4$ as analyzed by powder X-ray diffraction (Figure S1, Supporting Information).[13] This segregation of the two metals after heating may reflect an instability of HgCuS solids.[14] Consistent with these results, thermogravometric analysis of **1** (Figure 1) depicts three decomposition steps starting at 100 °C leading to a total of 78.6% mass loss by 440 °C and the formation of elemental mercury. This change in mass cannot be simply explained by the loss of the phosphine ligands, either as free PPr_3 (calcd 36.2%) or $S{=}PPr_3$ (calcd 43.5%). The visible generation of mercury metal and powder

(5) (a) Corrigan, J. F.; Fenske, D. *Chem. Commun.* **1997**, 1837−1838. (b) Corrigan, J. F.; Fenske, D. *Angew. Chem., Int. Ed. Engl.* **1997**, *36*, 1981−1983. (c) Langetepe, T.; Fenske, D. *Z. Anorg. Allg. Chem.* **2001**, *627*, 820−826. (d) Pfistner, H.; Fenske, D. *Z. Anorg. Allg. Chem.* **2001**, *627*, 575−582. (e) Semmelmann, M.; Fenske, D.; Corrigan, J. F. *J. Chem. Soc., Dalton Trans.* **1998**, 2541−2545. (f) Corrigan, J. F.; Balter, S.; Fenske, D. *J. Chem. Soc., Dalton Trans.* **1996**, 729−738.

(6) (a) Eichhöfer, A.; Fenske, D. *J. Chem. Soc., Dalton Trans.* **2000**, 941−944. (b) Li, H.; Kim, J.; Groy, T. L.; O'Keeffe, M.; Yaghi, O. M. *J. Am. Chem. Soc.* **2001**, *123*, 4867−4868. (c) Fenske, D.; Bettenhausen, M. *Angew. Chem., Int. Ed.* **1998**, *37*, 1291−1294.

(7) Lucas, C.; Amingual, D.; Chatard, J. P. *J. Phys. IV* **1994**, *4*, 177−182.

(8) (a) Czekelius, C.; Hilgendorff, M.; Spanhel, L.; Bedja, I.; Lerch, M.; Müller, G.; Bloeck, U.; Su, D.-S.; Giersig, M. *Adv. Mater.* **1999**, *11*, 643−646. (b) Kumar S. R. *Indian J. Pure Appl. Phys.* **1999**, *37*, 356−358. (c) Gurinovich, L. I.; Gurin, V. S.; Ivanov, V. A.; Bodnar, I. V.; Molochko, A. P.; Solovej, N. P. *Phys. Status Solidi B* **1998**, *208*, 533−540. (d) Klaer, J.; Bruns, J.; Henninger, R.; Seimer, K.; Klenk R.; Ellmer K.; Braunig, D. *Semicond. Sci. Technol.* **1998**, *13*, 1456−1458.

(9) Tran, D. T. T.; Taylor, N. J.; Corrigan, J. F. *Angew. Chem., Int. Ed.* **2000**, *39*, 935−937.

(10) Tran, D. T. T.; Corrigan, J. F. *Organometallics* **2000**, *19*, 5202−5208.

(11) (a) Bettenhausen, M.; Fenske, D. *Z. Anorg. Allg. Chem.* **1998**, *624*, 1245−1246. (b) Dean, P. A. W.; Vittal, J. J.; Wu, Y. *Inorg. Chem.* **1994**, *33*, 2180−2186. (c) Dean, P. A. W.; Manivannan, V. *Inorg. Chem.* **1990**, *29*, 2997−3002. (d) Dean, P. A. W.; Manivannan, V. *Can. J. Chem.* **1990**, *68*, 214−222. (e) Dean, P. A. W.; Vittal, J. J.; Trattner, M. H. *Inorg. Chem.* **1987**, *26*, 4245−4251. (f) Arnold, A. P.; Canty, A. J.; Skelton, B. W.; White, A. H. *J. Chem. Soc., Dalton Trans.* **1982**, 607−613. (g) Dean, P. A. W.; Manivannan, V.; Vittal, J. J. *Inorg. Chem.* **1989**, *28*, 2360−2368. (h) Singh, A. K.; Khandelwal, B. L.; Srivastava, V. *Phosphorus, Sulfur, Silicon Relat. Elem.* **1990**, *48*, 169−171. (i) Freedman, D.; Emge, T. J.; Brennan, J. G. *J. Am. Chem. Soc.* **1997**, *119*, 11112−11113.

(12) Behrens, S.; Bettenhausen, M.; Deveson, A. C.; Eichhöfer, A.; Fenske, D.; Lohde, A.; Woggon, U. *Angew. Chem., Int. Ed. Engl.* **1996**, *35*, 2215−2218.

(13) (a) Wells, A. F. *Structural Inorganic Chemistry*, 5th ed.; Oxford University Press: Toronto, Canada, 1984; pp 1142−1145.

(14) Charbonnier, M.; Murat, M. *Mater. Res. Bull.* **1972**, *7*, 1473−1483.

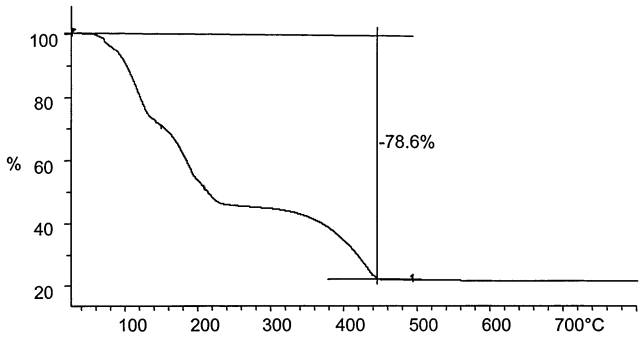

Figure 1. Thermogravimetric analysis curve for $[Hg_{15}Cu_{20}S_{25}(PPr_3)_{18}]$ (**1**).

X-ray diffraction (Figure S2, Supporting Information) indicate that the remaining crusty gray solid is a mixture of various forms of copper sulfide which include $Cu_{1.96}S$, $Cu_{1.81}S$, $Cu_{62}S_{32}$, $Cu_{1.9375}S$, Cu_2S, and $Cu_{7.2}S_4$.[13] A GC-MS analysis of the emitted volatiles (excluding mercury metal) from the TGA analysis revealed that it consisted of ∼15% tripropylphosphine and ∼85% of $S{=}PPr_3$. A calculated weight loss from **1** from the combined elimination of this ratio of phosphine/phosphine−sulfide and the mercury centers (80.0%) is in good agreement with the observed weight loss (78.6%). Thus, in addition to ligand elimination from the cluster surface during thermolysis, Hg(0) formation and elimination also occurs to yield various mixtures of Cu(I)/Cu(II)/S solids. Although this illustrates that complexes such as **1** may not be suitable precursors to related Hg^{II}-$Cu^{I}S_x$ solids due to the facile redox chemistry involved, it does demonstrate clearly the advantage of the low-temperature synthesis in achieving kinetically controlled mixing of the three core elements in the cluster complex.

In a similar manner as for the preparation of **1**, when $(Pr_3P)_3Cu{-}SeSiMe_3$ (**4b**) was reacted with tripropylphosphine-solubilized $Hg(OAc)_2$, ruby red crystals of $[Hg_{15}Cu_{20}Se_{25}(P\mathit{n}Pr_3)_{18}]$ (**2**) formed in high yield (>80%) within 24−48 h at low temperatures. As with **1**, the phosphine used to solubilize the mercury acetate does not affect the cluster product formed. Unlike its sulfide analogue **1**, cluster **2** is red in color when isolated and only darkens to a black color after several weeks of exposure to ambient light.

Data from single-crystal X-ray analysis illustrate that **2** is isostructural (and isomorphous) to **1,** and Table 1 summarizes the structural parameters for **2**. The cluster core in **2** is larger than is observed in **1**, 0.7 × 1.5 × 1.5 nm^3. The "flattened" nature of this cluster is illustrated in the projection of **2** (Figure 1). The molecule resides on a crystallographic $\bar{3}$ site with the 3-fold axis lying along the Hg2−Se5 vector. About the central selenide (Se5) there is some disorder, where in which the Hg3 and Cu3 are distributed over six equivalent sites. At any particular time there are two copper sites and one mercury site about Se5. The disorder is such that the relative occupancy of Cu3/Hg3 was satisfactorily refined as 2:1 (0.3333:0.16667). Copper centers (Cu1) are bonded to two phosphine ligands and exhibit tetrahedral coordination, and two other copper centers (Cu4, Cu5) are only singly coordinated to a tripropylphosphine ligand and also assume tetrahedral geometry. The internal copper centers (Cu2, Cu3) exhibit coordination numbers 3 and 4, respectively. Cu··· Cu and Hg···Hg contacts are ∼2.5 and 3.4 Å, respectively, which is consistent with oxidation states +1 (Cu) and +2 (Hg) for the d^{10} metals centers. The Hg atoms display either near-linear coordination (Hg1; −Se1−Hg1−Se2 = 179.41(7)°) or trigonal planar (Hg2, Hg3, Hg4, Hg5) geometry. The selenium atoms bridge the copper and mercury centers in μ_3 (Se5) or μ_4 (Se1, Se2, Se3, Se4) fashion. A total of 13 of the 25 Se^{2-} ligands in **2** form a nonbonded centered icosahedron (Se3−5 and their symmetry equivalents, Figure 3), the remaining selenium surrounding this central polyhedron. The Hg−Se distances are comparable to the Hg−S lengths in **1**, 2.230(3) Å (Hg5−Se3)−3.018(2) Å (Hg5−Se2). UV−vis analysis of **2** in the solid state displays a featureless absorption spectrum, with an onset of absorption at ∼800 nm.

All of our attempts at accessing a Hg−Cu−Te complex using the tellurium reagent $(Pr_3P)_3Cu{-}TeSiMe_3$ have been unsuccessful to date, as invariably only amorphous, black materials are produced. Surprisingly, the synthesis of ternary clusters using triethylphosphine analogues of the copper chalcogenolate reagents **4a**,**b** have also been unsuccessful to date in stabilizing HgCuS/Se complexes. Reaction conditions analogous to those used for the synthesis of **1** and **2** using the shorter chain triethlylphosphine ligands repeatedly lead to the formation of insoluble precipitates or the

Table 1. Bond Lengths (Å) and Angles (deg) for $[Hg_{15}Cu_{20}Se_{25}(PPr_3)_{18}]$ (**2**)[a]

Hg(1)−Se(1)	2.4383(17)	Se(2)−Cu(5)	2.487(4)
Hg(1)−Se(2)	2.4421(17)	Se(3)−Cu(5)	2.700(5)
Hg(2)−Se(3)	2.5895(18)	Se(4)−Cu(2)	2.394(3)
Hg(4)−Se(4)	2.341(2)	Se(4)−Hg(3)	2.524(5)
Hg(5)−Se(3)	2.230(3)	Se(4)−Cu(3)	2.643(13)
Hg(5)−Se(4)	2.329(2)	Se(4)−Cu(5)	2.666(4)
Hg(5)−Se(2)	3.018(2)	Se(4)−Cu(4)	2.716(4)
Se(1)−Cu(2)	2.423(3)	Se(5)−Hg(3)	2.350(5)
Se(1)−Cu(1)	2.606(3)	Se(5)−Cu(3A)	2.574(14)
Se(1)−Hg(1)−Se(2)	179.41(7)	Hg(2)−Se(3)−Cu(3)B	79.9(3)
Se(3)B−Hg(2)−Se(3)	118.941(18)	Cu(5)−Se(3)−Cu(3A)A	63.1(3)
Se(3)C−Hg(4)−Se(4)	147.36(11)	Hg(5)−Se(4)−Hg(4)	91.85(9)
Se(4)−Hg(4)−Se(1)D	103.59(8)	Hg(5)−Se(4)−Cu(2)	127.52(11)
Se(3)−Hg(5)−Se(4)	149.00(11)	Hg(4)−Se(4)−Cu(2)	126.88(10)
Se(3)−Hg(5)−Se(2)	101.69(8)	Hg(5)−Se(4)−Hg(3)	93.42(14)
Se(4)−Hg(5)−Se(2)	105.29(8)	Cu(2)−Se(4)−Hg(3)	87.0(2)
Cu(2)−Se(1)−Hg(1)	86.19(8)	Cu(3)−Se(4)−Hg(3)A	67.2(3)
Cu(2)−Se(1)−Cu(4)A	83.24(12)	Hg(4)−Se(4)−Cu(5)	98.36(11)
Cu(2)−Se(1)−Cu(1)	60.54(8)	Hg(3)A−Se(4)−Cu(5)	84.8(2)
Hg(1)−Se(1)−Cu(1)	112.98(8)	Hg(5)−Se(4)−Cu(3A)	100.0(3)
Cu(4)A−Se(1)−Cu(1)	134.02(13)	Hg(4)−Se(4)−Cu(3A)	70.9(4)
Cu(2)−Se(1)−Hg(4)A	58.58(8)	Hg(3)A−Se(4)−Cu(3A)	49.5(3)
Cu(1)−Se(1)−Hg(4)A	117.01(8)	Hg(5)−Se(4)−Cu(3A)A	36.8(4)
Cu(2)A−Se(2)−Hg(1)	85.61(8)	Cu(2)−Se(4)−Cu(3A)A	101.6(4)
Cu(2)A−Se(2)−Cu(5)	84.95(12)	Cu(5)−Se(4)−Cu(3)A	101.5(4)
Hg(1)−Se(2)−Cu(5)	89.11(11)	Hg(5)−Se(4)−Cu(4)	98.34(11)
Hg(1)−Se(2)−Cu(1)A	110.87(8)	Cu(5)−Se(4)−Cu(4)	88.45(13)
Cu(2)A−Se(2)−Hg(5)	60.81(7)	Cu(3A)−Se(4)−Cu(4)	100.3(4)
Hg(1)−Se(2)−Hg(5)	78.18(5)	Cu(3A)A−Se(4)−Cu(4)	114.2(4)
Cu(1)A−Se(2)−Hg(5)	120.03(8)	Cu(3)A−Se(4)−Cu(4)	132.3(3)
Hg(4)B−Se(3)−Hg(5)	93.70(10)	Hg(3)−Se(5)−Hg(3)A	60.065(17)
Hg(5)−Se(3)−Hg(2)	93.64(9)	Hg(3)−Se(5)−Cu(3A)B	126.5(3)
Hg(5)−Se(3)−Cu(4)B	117.70(13)	Hg(3)a−Se(5)−Cu(3A)	53.5(3)
Hg(4)B−Se(3)−Cu(5)	116.82(12)	Cu(3A)E−Se(5)−Cu(3A)	180.0(11)
Hg(2)−Se(3)−Cu(5)	109.11(12)	Cu(3A)B−Se(5)−Cu(3A)	111.9(4)
Cu(4)B−Se(3)−Cu(5)	128.83(14)	Hg(3)−Se(5)−Cu(3A)C	53.5(3)
Hg(5)−Se(3)−Cu(3)B	68.4(3)		

[a] Symmetry transformations used to generate equivalent atoms: A, $x-y, x, -z$; B, $-y, x-y, z$; C, $-x+y, -x, z$; D, $y, -x+y, -z$; E, $-x, -y, -z$.

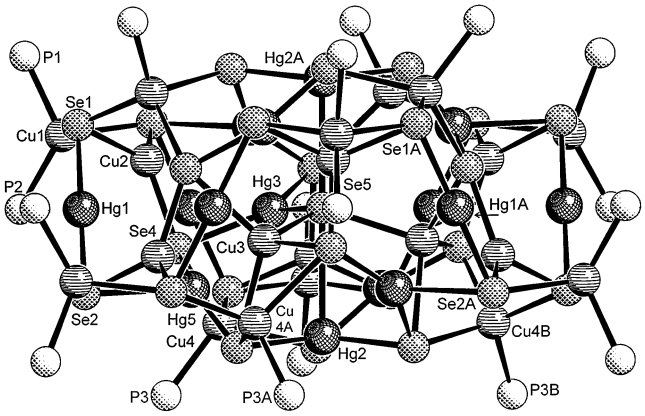

Figure 2. Molecular structure of $[Hg_{15}Cu_{20}Se_{25}(PPr_3)_{18}]$ (**2**). Carbon atoms about the phosphorus centers have been omitted for clarity.

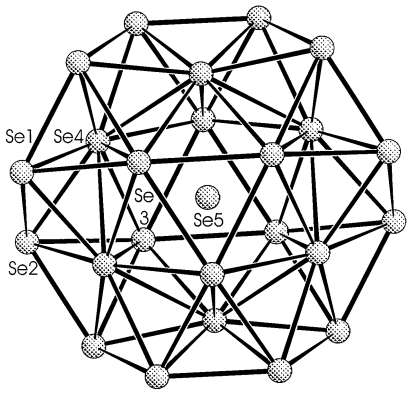

Figure 3. Nonbonded Se_{25} polyhedron in **2**.

decomposition of the reagent and subsequent formation of elemental selenium or tellurium.

The recent report by Eichhöfer and Fenske of CuInSe clusters using a mixture of phosphine-solubilized CuCl:$InCl_3$ salts and $Se(SiMe_3)_2$ prompted us to explore the suitability of reagents $(R_3P)Cu-SSiMe_3$ for the synthesis of Cu−In−S cluster complexes. The first copper−indium−sulfur (thiolate) cluster was reported by Kanatzidis and co-workers,[15a] $[Cu_6In_3(SEt)_{16}]^-$ (**I**), in an attempt to use it as a precursor to $CuInS_2$. The same group was then successful in a subsequent attempt, in making $[(Ph_3P)_2CuIn(\mu\text{-}E-Et)_4]$ (E = Se, S), the first single-source precursor to $CuInE_2$.[15b]

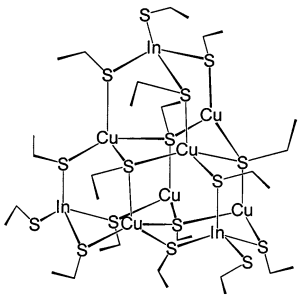

I

The reaction of a 3:1 ratio of **5**:$InCl_3$ leads to trace amounts of $[Cu_6In_8Cl_4S_{13}(PEt_3)_{12}]$ (**3**) as the only crystalline product.

(15) (a) Hirpo, W.; Dhingra, S.; Kanatzidis, M. G. *J. Chem. Soc., Chem. Commun.* **1992**, 557−558. (b) Hirpo, W.; Dhingra, S.; Sutorik, A. C.; Kanatzidis, M. G. *J. Am. Chem. Soc.* **1993**, *115*, 1597−1599.

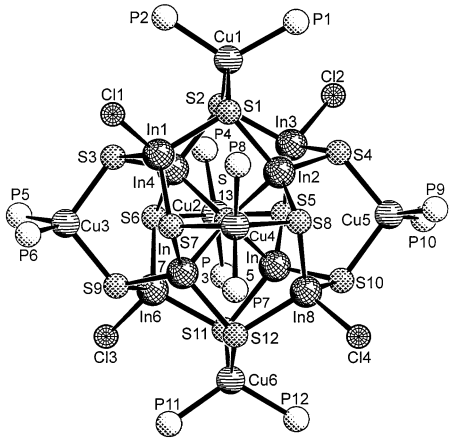

Figure 4. Molecular structure of $[Cu_6In_8S_{13}Cl_4(PEt_3)_{12}]$ (**3**). Carbon atoms about the phosphorus centers have been omitted for clarity.

The yield of **3** can be markedly improved (50%) however by providing an additional source of sulfide ligands, in the form of $S(SiMe_3)_2$, according to eq 2:

$$8InCl_3 + 6(PEt_3)_3Cu-SSiMe_3\ (\mathbf{5}) + 7S(SiMe_3)_2 \rightarrow [Cu_6In_8Cl_4S_{13}(PEt_3)_{12}]\ (\mathbf{3}) + 20ClSiMe_3 + 6PEt_3 \quad (2)$$

Small crystals of **3** were grown from pentane−THF mixtures at −5 °C. Repeated attempts at growing larger samples were unsuccessful, and thus, the diffraction data are weak. In addition, crystals of **3** desolvate rapidly once removed from their mother liquor. Both of these factors contribute to the rather poor quality of the X-ray data; however, the structure of **3** could be satisfactorily solved and refined (Tables 2 and 3). The structure of this molecule is markedly different from that observed in the copper−indium−sulfur cluster,[15a] **I**. The structure of **3** (Figure 4) does not display any adamantoid structural characteristics as observed in $[Cu_6In_3(SEt)_{16}]^-$, which contains (surface) thiolate ligands. Thus, while the Cu_6In_3 cluster is described as having a central $[Cu_6S_4]$ core, **3** has an inner $[In_8S_{13}]$ framework. The structure of **3** is very similar to that of two recently reported copper−indium−selenide clusters $[Cu_6In_8Se_{13}Cl_4(PPh_3)_6(CH_8O)]$ and $[Cu_6In_8Se_{13}Cl_4(P^nPr_2Ph)_{12}]$ **(II)**.[6a] The $[In_8S_{13}]$ core has a central sulfur atom, S13, that is coordinated to four inner indium centers (In2, In4, In5, In7) in a distorted tetrahedral geometry (−In−S13−In 108.4(3)−111.0(3)°). These inner indium centers are each bonded to three additional sulfur atoms, which themselves are also bonded to the four outer (In1, In3, In6, In8) indium centers. The two sets of inner and outer indium centers (In2, In4, In5, In7 and In1, In3, In6, In8) are each arranged to form In_4 tetrahedra. The 12 outer sulfur centers (S1−S12) act as μ_3-ligands, each bonded to two indium centers and one $Cu(PEt_3)_2$ unit. The In−S bonds of the inner indium centers to these sulfur ligands (Table 3) range from 2.394(9) to 2.454(9) Å in length. These bonds are observed to be slightly shorter than the $In-S_{12}$ bonds of the outer indium centers, which range from 2.425(10) to 2.473(9) Å. The In−S contacts to the central sulfur, S13, are even longer at 2.541(8)−2.559(8) Å. The outer S1−S12 centers are arranged such that they form a distorted (nonbonded) icosahedral arrange-

Table 2. Selected Bond Lengths (Å) and Angles (deg) for $[Cu_6In_8S_{13}Cl_4(PEt_3)_{12}]$ (**3**)

In(1)−Cl(1)	2.403(9)	In(6)−S(6)	2.454(9)
In(1)−S(7)	2.453(8)	In(7)−S(9)	2.430(9)
In(1)−S(3)	2.455(8)	In(7)−S(7)	2.437(8)
In(1)−S(1)	2.459(9)	In(7)−S(11)	2.452(9)
In(2)−S(8)	2.394(9)	In(7)−S(13)	2.559(8)
In(2)−S(1)	2.440(8)	In(8)−Cl(4)	2.426(11)
In(2)−S(4)	2.454(8)	In(8)−S(10)	2.465(9)
In(2)−S(13)	2.553(8)	In(8)−S(8)	2.473(9)
In(3)−S(5)	2.425(10)	In(8)−S(11)	2.473(9)
In(3)−Cl(2)	2.428(9)	Cu(1)−S(1)	2.368(9)
In(3)−S(2)	2.433(8)	Cu(1)−S(2)	2.443(9)
In(3)−S(4)	2.454(8)	Cu(2)−S(5)	2.407(10)
In(4)−S(3)	2.402(8)	Cu(2)−S(6)	2.415(10)
In(4)−S(2)	2.427(8)	Cu(3)−S(9)	2.410(9)
In(4)−S(6)	2.439(8)	Cu(3)−S(3)	2.429(9)
In(4)−S(13)	2.558(7)	Cu(4)−S(7)	2.341(9)
In(5)−S(10)	2.416(9)	Cu(4)−S(8)	2.474(9)
In(5)−S(5)	2.435(9)	Cu(5)−S(4)	2.402(9)
In(5)−S(12)	2.454(9)	Cu(5)−S(10)	2.431(9)
In(5)−S(13)	2.541(8)	Cu(6)−S(12)	2.355(10)
In(6)−Cl(3)	2.403(11)	Cu(6)−S(11)	2.413(9)
In(6)−S(9)	2.428(10)		
In(6)−S(12)	2.443(9)		

Cl(1)−In(1)−S(7)	102.9(3)	S(3)−In(4)−S(6)	115.6(3)
Cl(1)−In(1)−S(3)	105.1(3)	S(2)−In(4)−S(6)	116.2(3)
S(7)−In(1)−S(3)	115.8(3)	S(3)−In(4)−S(13)	102.6(3)
Cl(1)−In(1)−S(1)	107.5(3)	S(2)−In(4)−S(13)	101.7(3)
S(7)−In(1)−S(1)	113.3(3)	S(6)−In(4)−S(13)	100.3(3)
S(3)−In(1)−S(1)	111.3(3)	S(10)−In(5)−S(5)	116.8(3)
S(8)−In(2)−S(1)	115.7(3)	S(10)−In(5)−S(12)	116.0(3)
S(8)−In(2)−S(4)	118.2(3)	S(5)−In(5)−S(12)	116.9(3)
S(1)−In(2)−S(4)	114.4(3)	S(10)−In(5)−S(13)	101.8(3)
S(8)−In(2)−S(13)	103.1(3)	S(5)−In(5)−S(13)	100.5(3)
S(1)−In(2)−S(13)	100.0(3)	S(12)−In(5)−S(13)	100.1(3)
S(4)−In(2)−S(13)	101.4(3)	Cl(3)−In(6)−S(9)	106.8(4)
S(5)−In(3)−Cl(2)	105.0(3)	Cl(3)−In(6)−S(12)	103.4(4)
S(5)−In(3)−S(2)	114.4(3)	S(9)−In(6)−S(12)	112.5(3)
Cl(2)−In(3)−S(2)	104.3(3)	Cl(3)−In(6)−S(6)	105.3(4)
S(5)−In(3)−S(4)	113.3(3)	S(9)−In(6)−S(6)	112.2(3)
Cl(2)−In(3)−S(4)	105.3(3)	S(12)−In(6)−S(6)	115.6(3)
S(2)−In(3)−S(4)	113.3(3)	S(9)−In(7)−S(7)	115.8(3)
S(3)−In(4)−S(2)	116.5(3)	S(9)−In(7)−S(11)	117.6(3)
S(7)−In(7)−S(11)	115.5(3)	Cu(2)−S(5)−In(5)	108.8(4)
S(9)−In(7)−S(13)	100.2(3)	In(3)−S(5)−In(5)	99.7(3)
S(7)−In(7)−S(13)	101.0(3)	Cu(2)−S(6)−In(4)	108.4(3)
S(11)−In(7)−S(13)	102.4(3)	Cu(2)−S(6)−In(6)	110.5(4)
Cl(4)−In(8)−S(10)	106.0(4)	In(4)−S(6)−In(6)	99.8(3)
Cl(4)−In(8)−S(8)	105.0(4)	Cu(4)−S(7)−In(7)	110.9(3)
S(10)−In(8)−S(8)	112.7(3)	Cu(4)−S(7)−In(1)	112.6(3)
Cl(4)−In(8)−S(11)	106.2(4)	In(7)−S(7)−In(1)	99.1(3)
S(10)−In(8)−S(11)	112.2(3)	In(2)−S(8)−In(8)	98.8(3)
S(8)−In(8)−S(11)	114.0(3)	In(2)−S(8)−Cu(4)	109.5(4)
S(1)−Cu(1)−S(2)	104.3(3)	In(8)−S(8)−Cu(4)	110.9(3)
S(5)−Cu(2)−S(6)	105.6(3)	Cu(3)−S(9)−In(6)	113.3(4)
S(9)−Cu(3)−S(3)	105.8(3)	Cu(3)−S(9)−In(7)	109.0(3)
S(7)−Cu(4)−S(8)	104.1(3)	In(6)−S(9)−In(7)	99.1(3)
S(4)−Cu(5)−S(10)	105.2(3)	In(5)−S(10)−Cu(5)	107.3(4)
P(11)−Cu(6)−P(12)	113.4(5)	In(5)−S(10)−In(8)	100.2(3)
S(12)−Cu(6)−S(11)	105.2(3)	Cu(5)−S(10)−In(8)	113.8(3)
Cu(1)−S(1)−In(2)	108.4(3)	Cu(6)−S(11)−In(7)	107.1(3)
Cu(1)−S(1)−In(1)	116.6(3)	Cu(6)−S(11)−In(8)	113.3(3)
In(2)−S(1)−In(1)	99.3(3)	In(7)−S(11)−In(8)	98.4(3)
In(4)−S(2)−In(3)	99.1(3)	Cu(6)−S(12)−In(6)	114.1(4)
In(4)−S(2)−Cu(1)	109.3(3)	Cu(6)−S(12)−In(5)	110.2(4)
In(3)−S(2)−Cu(1)	109.4(3)	In(6)−S(12)−In(5)	98.9(3)
In(4)−S(3)−Cu(3)	108.6(3)	In(5)−S(13)−In(2)	108.4(3)
In(4)−S(3)−In(1)	98.9(3)	In(5)−S(13)−In(4)	111.0(3)
Cu(3)−S(3)−In(1)	109.0(3)	In(2)−S(13)−In(4)	109.4(3)
Cu(5)−S(4)−In(3)	110.9(3)	In(5)−S(13)−In(7)	108.8(3)
Cu(5)−S(4)−In(2)	108.2(3)	In(2)−S(13)−In(7)	109.0(3)
In(3)−S(4)−In(2)	99.2(3)	In(4)−S(13)−In(7)	110.2(3)
Cu(2)−S(5)−In(3)	111.9(4)		

Table 3. Crystallographic Data for the Structure Determinations of **1**−**3**

param	**1**	**2**	**3**
chem formula	$C_{162}H_{378}Cu_{20}Hg_{15}P_{18}S_{25}$	$C_{162}H_{378}Cu_{20}Hg_{15}P_{18}Se_{25}$	$C_{72}H_{180}Cl_4Cu_6In_8P_{12}S_{13}$
fw	7965.25	9137.75	3276.18
space group	$R\bar{3}$	$R\bar{3}$	$I\bar{4}2d$
temp (°C)	−73	−73	−73
a (Å)	23.5814(9)	23.7830(6)	38.2199(7)
c (Å)	43.376(2)	43.2493(9)	36.9701(7)
α (deg)	90	90	90
β (deg)	90	90	90
γ (deg)	120	120	90
V (Å^3)	20 889.1(15)	21 185.7(9)	54 004.5(17)
μ (Mo Kα_1, mm^{-1})	10.044	12.940	2.714
Z	3	3	16
ρ_c (g cm^{-3})	1.900	2.149	1.612
data:params	2586:300	5769:314	13 527:672
R indices [$I > 2\sigma(I)$][a]	$R_1 = 0.0709$ $wR_2 = 0.2167$	$R_1 = 0.0746$ $wR_2 = 0.2094$	$R_1 = 0.1118$ $wR_2 = 0.2831$

[a] $R_1 = \Sigma||F_o| - |F_c||/\Sigma|F_o|$. $wR_2 = \{\Sigma[w(F_o^2 - F_c^2)^2/\Sigma[wF_o^2]^2]\}^{1/2}$.

ment. The four inner indium centers are positioned below the triangular faces of the icosahedron, while the four chlorine-bonded indium atoms lie above S_3 faces of the defined S_{12} polyhedron. The 12 surface PEt_3 and 4 Cl ligands stabilize the inner 1.0 × 1.0 × 1.0 nm^3 core.

The UV spectrum for a solution of **3** displays a weak maximum at 400 nm, with the onset of absorption at 490 nm, mirroring observations for the related selenium complex $[Cu_6In_8Se_{13}Cl_4(PPh_3)_6(OC_4H_8)]$.[6a] Solid-state diffuse reflectance spectra of **3** display a similar profile.

Conclusions

We have demonstrated that tris(trialkylphosphine)copper(I)−(trimethylsilyl)chalcogenolates (E = S, Se)[10] may be used for the synthesis of ternary nanoclusters. The reaction of **4a,b** with mercury(II) acetate led to the isolation of the pinwheel-shaped complexes $[Hg_{15}Cu_{20}E_{25}(PnPr_3)_{18}]$ (E = S, Se) (**1** and **2**), respectively. The cluster $[Cu_6In_8S_{13}Cl_4(PEt_3)_{12}]$ (**3**) can be similarly prepared from the reaction of **5** and $InCl_3$ although the yields are improved dramatically if additional amounts of $S(SiMe_3)_2$ are used.

Experimental Section

Experiments were all performed in an inert nitrogen atmosphere with the use of Schlenk line techniques and gloveboxes. Complexes **4** and **5** were synthesized as described.[10] PPr_3[16] and $S(SiMe_3)_2$[17] were prepared and purified as reported in the literature. $Hg(OAc)_2$ and $InCl_3$ were purchased from Strem Chemical at 99.99% purity and used as supplied. Solvents were obtained from Caledon and BDH Chemicals and subsequently dried and distilled over sodium/benzophenone (Et_2O, THF) or P_2O_5 (CH_3CN). Nuclear magnetic resonance spectroscopy experiments were measured on Gemini 300 (^{1}H, 300.075 MHz; ^{13}C{^{1}H}, 75.4 MHz) and Varian Mercury 400 (^{1}H, 400.088 MHz; ^{13}C{^{1}H}, 100.613 MHz; ^{31}P{^{1}H}, 161.957 MHz) spectrometers. ^{1}H and ^{13}C{^{1}H} NMR spectra were measured using standard settings and chemical shifts were reported in ppm and externally referenced to $SiMe_4$ (using the residual protons and the

(16) Cumper, C. W. N.; Foxton, A. A.; Read, J.; Vogel, A. I. *J. Chem. Soc.* **1964**, 430.
(17) (a) Schmidt, V. H.; Ruf, H. *Z. Anorg. Allg. Chem.* **1963**, *321*, 270. (b) So, J.; Boudjouk, P. *Synthesis* **1989**, 306.

carbons of the deuterated solvent, respectively). $^{31}P\{^{1}H\}$ spectra were referenced externally to 85% phosphoric acid with the 90° pulse width at 16 μs, using a 16 μs pulse, a 0.4 s acquire time, and a 1 s delay time. Chemisar Laboratories Inc. (Guelph, Ontario, Canada) performed chemical analyses. GC-MS analysis was performed on a Finnigan MAT 8200 mss-data system. Gas chromatography was performed with an injector temperature of 225 °C and a 30 m DB5 MS column. The UV−vis spectra were obtained on a Varian Cary 100 Bio UV−vis spectrophotometer. An additional module was used to measure solid-phase diffuse reflectance spectra, and spectra were collected as the percent reflectance of a sample diluted in dried KBr. Thermogravometric analysis (TGA) was performed on a Mettler Toledo TGA SDTA851[e] with included software and a constant nitrogen purge. The volatiles were collected through vinyl tubing into a Schlenk tube immersed in a cold trap of liquid nitrogen.

Synthesis of $[Hg_{15}Cu_{20}S_{25}(PPr_3)_{18}]$ (1). Mercury(II) acetate (0.63 g, 2.0 mmol) was dissolved in 15 mL of cold (∼−30 °C) tetrahydrofuran with tripropylphosphine (0.64 mL, 4.0 mmol) to give a clear colorless solution. The mercury acetate solution was cooled to −75 °C and added to a solution of **4a** (2.66 g, 4.0 mmol) in 10 mL of THF at −75 °C. The reaction mixture turned bright yellow in color and became bright orange upon warming to −30 °C. Orange crystalline blocks of **1**, suitable for X-ray analysis (0.62 g, 60% based on Hg), appeared within ∼48 h at −30 °C. Anal. Calcd: C, 24.43; H, 4.78. Found: C, 24.43; H, 4.57.

Synthesis of $[Hg_{15}Cu_{20}Se_{25}(PPr_3)_{18}]$ (2). $[Hg_{15}Cu_{20}Se_{25}(P\mathit{n}Pr_3)_{18}]$-(**2**) was prepared in a similar procedure as used for **1**: $Hg(OAc)_2$ (0.77 g, 2.4 mmol) was dissolved in 20 mL of THF with PPr_3 (0.96 mL, 4.8 mmol). Once completely dissolved, this clear solution was cooled to −75 °C and added to a cold solution of **4b** dissolved in 40 mL of THF at the same temperature. Upon mixing, the reaction mixture immediately became clear, bright orange and was warmed slowly to −30 °C. Within ∼48 h, ruby red crystals of **2**, suitable for X-ray analysis, formed from a pale orange solution. Yield: 1.23 g (84% based on Hg).

Anal. Calcd: C, 21.29; H, 4.17; P, 6.10. Found: C, 22.70; H, 4.54; P, 6.41.

Preparation of $[Cu_6In_8S_{13}Cl_4(PEt_3)_{12}]$ (3). $InCl_3$ (0.07 g, 0.3 mmol) was dissolved in 10 mL of tetrahydrofuran, resulting in a clear, colorless solution. After the $InCl_3$ solution was cooled to −65 °C, it was added to a cold (−65 °C) solution of $(PEt_3)_3CuSSiMe_3$ (**5**) (0.12 g, 0.225 mmol) in 5 mL of tetrahydrofuran. $S(SiMe_3)_2$ (0.06 mL, 0.263 mmol) was then added, and the reaction solution was allowed to warm to −25 °C for 12 h. White powder precipitated, and the solution became slightly colored overnight. After several hours at room temperature, the precipitate redissolved and the solution became yellow in color. X-ray-quality, pale yellow crystals of **3** formed by layering solutions with pentane (5:2 C_5H_{12}−OC_4H_8) and cooling to −5 °C. Yield: 0.06 g (50%).

^{1}H NMR (CD_3CN, δ): 1.6 [br, 2H, CH_2], 1.1 [d of t, $^{3}J_{HH} = 7.2$ Hz, $^{3}J_{HP} = 14.6$ Hz, 3H, CH_3]. $^{31}P\{^{1}H\}$ NMR (CD_3CN, δ): −13.0 [s, br]. Anal. Calcd: C, 26.40; H, 5.54. Found: C, 25.9; H, 5.48.

X-ray Crystallographic Analysis of 1−3. Crystals were mounted immersed in cold mineral oil and placed in a cold stream of N_2 during data collection. Single crystals of **1**−**3** suitable for X-ray analysis were mounted on glass fibers. Data were collected using a Nonius Kappa-CCD diffractometer running the COLLECT (Nonius, 1998) software. Unit cell parameters were calculated and refined from the full data set. Crystal cell refinement and data reduction were carried out with the Nonius DENZO package. The data were scaled using SCALE-PACK (Nonius, 1998), and no other absorption corrections were applied. The SHELXTL (G. M. Sheldrick, Madison, WI) program package was applied to solve (direct methods) and refine the structure. All metal and phosphorus atoms (with the exception of the disordered P and C atoms) were refined with anisotropic thermal parameters, and carbon atoms were refined isotropically. A summary of the X-ray crystallographic data can be found in Table 3. Crystals of **3** appeared to desolvate rapidly, and this, in conjunction with the small sample size of the crystal (0.001 mm^3), subsequently affected the quality of the X-ray data. Although the structure of **3** was successfully solved in the noncentrosymmetric space group *I*42*d*, highly disordered ethyl ligands about the phosphorus centers prohibited the location of all C atoms to be determined in the difference Fourier map. Two data sets were collected for **3**, and the better of the two was used for the solution and refinement of **3**. The absolute structure parameter (0.51(5)) was refined using the SHELX "TWIN" command. Attempts to solve the structure in centrosymmetrical space groups (*I*4/*m*, *I*4/*mmm*) were unsuccessful. Figures of **1**−**3** were generated using the SCHAKAL 99 drawing program.[18]

Powder X-ray Diffraction Analysis. Powder XRD measurements were done on an Inel diffractometer equipped with XRG 3000 generator and CPS 120 curved position sensitive detector using monochromated Cu $K\alpha_1$ radiation ($\lambda = 1.540\,56$ Å), as thin films. The accompanying software was used for peak searches and indexing.

Acknowledgment. We are grateful to the Natural Sciences and Engineering Research Council of Canada and the Government of Ontario's Premier's Research Excellence Award program (to J.F.C.) for supporting this research. We also acknowledge the Canada Foundation for Innovation, the Ontario Research and Development Challenge Fund, and The University of Western Ontario's ADF program for equipment funding.

Supporting Information Available: X-ray crystallographic files in CIF format for clusters $[Hg_{15}Cu_{20}S_{25}(PPr_3)_{18}]$ (**1**), $[Hg_{15}Cu_{20}Se_{25}(PPr_3)_{18}]$ (**2**), and $[Cu_6In_8S_{13}Cl_4(PEt_3)_{12}]$ (**3**), a powder diffraction pattern for the residue of **1** after thermal treatment to 110 °C (Figure S1), a powder diffraction pattern for the residue of **1** after thermal treatment to 900 °C (Figure S2), and a projection of the disorder of the central core in **2** (Figure S3). This material is available free of charge via the Internet at http://pubs.acs.org.

IC0110528

(18) Keller, E. *SCHAKAL 1999, A Computer Program for the Graphic Representation of Molecular and Crystallographic Models*; Universität Freiburg: Freiburg, Germany, 1999.